Chapter 7

Modification of an Operational Dispersion Model for Urban Applications*

Abstract—An operational multi-source, multi-receptor Gaussian dispersion model, the Danish regulatory model OML, has been modified for applications in urban environments. A so-called roughness sublayer has been introduced into the model to represent the turbulence characteristics of the lowest part of the surface layer over rough surfaces like cities. The meteorological preprocessor was enhanced to take into account an urban energy budget. The performance of the resulting OML-Urban has been validated for NO_x and SO_2 for the city of Zurich for the year 1990. For this year, a detailed emission inventory as well as continuous hourly measurements at four stations are available. The air pollution monitoring stations used for validation have been divided into different groups, depending on local influences from nearby roads. The urban modification (roughness sublayer and changes in the met. preprocessor) results in a 25–35% increase of the annual mean surface concentration. OML-Urban shows a good reproduction of the probability density function of predicted concentrations, and the simulated yearly averaged concentrations show a good correspondence to observations.

Key words: dispersion modeling, urban turbulence, rough surfaces, urban air pollution, roughness sublayer

7.1 INTRODUCTION

Air pollution modeling in urban areas is different from the traditional single high stack source dispersion problem in many ways. The air pollution level in agglomerations often is dominated by a countless number of small, not well determined emission sources. The inhomogeneity of the built-up area often causes concentration measurements to be

* this chapter will be submitted for publication in *J. Appl. Met.*:
de Haan, P., Rotach, M. W., and Werfeli, M.: Modification of an operational dispersion model for urban applications.

locally influenced. Almost all emission sources and (human) receptors are situated within the lowest tens of meters.

Although crucial to micro-scale dispersion modeling, relatively little is known concerning the flow and turbulence structure over built-up areas. Irregularly spaced tall roughness elements such as buildings induce a roughness sublayer (RS), which ranges from ground-level to several times the average building height (Raupach *et al*. 1991), as displayed in Figure 1. The existence of a roughness sublayer is not specific to urban surfaces but, unlike to the case of smoother terrain, its vertical extension cannot be neglected. Within this RS the flow and turbulence fields are different from that of the surface layer above (Högström *et al.* 1982; Rotach 1993a, b, 1997b; Roth and Oke 1993; Roth 1993; Oikawa and Meng 1995).

Gaussian plume models represent a valid (analytical) solution to the diffusion equation only for idealized circumstances. Stationarity and homogeneity of the turbulence characteristics are requested. In practice, none of these conditions is fully satisfied, but Gaussian plume dispersion models have been successfully used for rural configurations. Extensive validation has been done on tracer experiments conducted e.g. in Kincaid and Prairie Grass (see e.g. Olesen 1995; Carruthers *et al.* 1992). Gaussian plume models have also been tested against tracer experiments in urban surroundings like the Indianapolis experiment (Hanna and Chang 1993). Especially, for the prediction of yearly averaged concentration based on hourly meteorological data, Gaussian plume models are still the method of choice. Also, Gaussian plume dispersion models have been applied to multi-source, multi-receptor situations in inhomogeneous urban environments (e.g. Gryning and Lyck 1984; Häggkvist 1997; Härkönen *et al.* 1998).

The question addressed in this paper is which changes should be made in order to apply Gaussian plume models to urban environments:

1. changes to the computing code of the dispersion model and its meteorological pre-processor (to take into account the turbulence characteristics and the energy balance over urban surfaces)
2. changes in the set-up of the model (emission height of sources and receptor heights within the urban canopy layer)

3. changes in model validation by classifying measuring sites into different groups depending on the influence of nearby roads and building structures.

Rotach (1997a) proposed a method to introduce the RS into dispersion models by using an 'urban meteorological preprocessor'. Since one of the main characteristics of a RS is the fact that the turbulent fluxes are not constant with height, the urban meteorological preprocessor allows for a non-constant Reynolds stress in the RS. This leads to higher wind speeds as compared with a logarithmic wind-profile (Rotach 1993a), and the concept of local scaling is used to determine turbulence statistics such as velocity variances (Rotach 1993b). If the dispersion model uses similarity theory instead of stability classes, the concept of local scaling within the RS needs to be implemented in the dispersion model itself. The parameterizations on urban stability and urban heat balance affect the meteorological pre-processor only.

The treatment of the Roughness Sublayer (RS) after Rotach (1997a) proved to be successful in improving the performance of dispersion models: For a Lagrangian stochastic particle model, Rotach and de Haan (1997) showed that the OML underprediction of surface concentrations for the Copenhagen tracer experiment vanishes (Olesen 1995). De Haan *et al.* (1998) introduced the RS concept into an operational Gaussian dispersion model (which is much more suited to handle multi-source, multi-receptor problems), the Danish regulatory model OML (cf. section 7.2.1). A similar performance improvement for the Copenhagen and, in addition, for the Lillestrøm tracer data set has been achieved.

The present contribution focuses on this modified version of the OML with an urban pre-processor, hereafter called 'OML-Urban', and presents the application to an entire city. The concept of the RS and other necessary changes to the OML meteorological pre-processor and dispersion model are presented (sections 7.2.2 and 7.2.3). The resulting OML-Urban is validated using an extensive data set from the city of Zurich. Measurements of NO_x and SO_2 are available at 28 different sites, which are divided into groups of different quality (section 7.3). It is shown that the concept of the urban modification leads to a clear improvement of the predictions of the OML model. The resulting simulated surface concentrations are very accurate (section 7.4).

7.2 ADAPTATION OF THE OML DISPERSION MODEL TO URBAN CONDITIONS

7.2.1 OML dispersion model

The so-called OML (Operationelle Meteorologiske Luftkvalitetsmodeller) is the basic atmospheric dispersion model for environmental impact assessments in Denmark. Besides the scientific multi-source/multi-receptor version used in the present work, OML-Multi, a single-source version for regulatory purposes is available (OML-Point). The OML is a Gaussian plume model, but in contrast to many regulatory models its physical description is not based on the traditional discrete stability categories (Pasquill-Turner stability classes). Instead, the model uses basic boundary layer scaling parameters (see below).

The OML is intended to be used for distances up to about 20 km from the source. It requires information on emission and meteorology on an hourly basis, and returns a time series of concentrations calculated at user-specified receptor points. For a more detailed description of the model see Olesen *et al.* (1992). The lower boundary of the model domain in the vertical direction equals the roughness length, z_0. Perfect reflection without deposition is assumed. This is done by placing a mirror source below the ground.

The meteorological preprocessor accompanying the OML is based on the resistance method (Berkowicz and Prahm 1982a). The method used is one-dimensional, i. e. neglecting heterogeneous surface conditions and topography. A description can be found in Olesen and Brown (1992).

7.2.2 Characteristics of the Roughness Sublayer

Within this RS the flow and turbulence structure is different from that of the surface layer, which latter usually constitutes the lowest part of applied (operational) dispersion models. The most striking difference is the fact that the turbulent fluxes of momentum (and heat) are not constant with height (cf. the identification of the surface layer as a ‘constant flux layer’): observations show an increase of the Reynolds Stress, τ, with

height (Rotach 1993a; Oikawa and Meng 1995; Feigenwinter *et al.* 1998; Rafailidis 1997). The non-constant Reynolds stress within the RS leads to a smaller gradient of mean wind speed as compared to the 'logarithmic profile' of the surface layer (Rotach 1993a) and the necessity to revise the scaling concept for the turbulence statistics such as velocity variances (Rotach 1993b). Instead of using a constant value of the friction velocity to scale velocity variances, within the RS Rotach (1993b) uses local scaling with the height-dependent friction velocity.

Both these features are likely to modify dispersion characteristics and hence surface concentrations over urban surfaces, and this modification may be severe due to the relatively large vertical extension of an urban RS:

- Within the meteorological pre-processor, for all observed friction velocity values from measurements within the RS, a 'reference' friction velocity, u_{*r}, representative for the inertial sublayer (IS) is computed (Rotach 1993a, his eq. (16))
- In the dispersion model, velocity variances are scaled with u_{*r} in the IS. In the RS below, a height dependent local friction velocity $u_*(z)$ is used (again using Eq. (16) from Rotach (1993a)). The same local scaling approach applies to the mean wind speed profile within the RS.

7.2.3 Introduction of an urban energy balance into the meteorological pre-processor

In this section, the modification of the original meteorological preprocessor of the OML (Olesen and Brown 1992) to take into account an urban energy budget is described. Meteorological preprocessing usually makes use of parameterizations based on measurements in rural environments. The main differences between rural, vegetated and surfaces of cities are a reduced evaporation, because of the fast run-off and built-up areas, and a limited storage capacity for water. This causes the latent heat flux to be much smaller as compared to rural environments. Furthermore, the roughness is much higher as compared to rural surfaces, often comparable to the roughness of forests.

The meteorological preprocessor accompanying the OML computes descriptive surface turbulence parameters using the resistance method of Berkowicz and Prahm (1982). The parameters are heat flux, friction velocity, Obukhov length and net radiation. The resistance method assumes analogy with Ohm's law when accounting for, on the one

hand, the resistance of the surface to evaporation, and on the other hand, the flux of heat and water vapor through the surface layer. Parameters have to be determined from data for the description of the stomatal resistance. This has been done in Berkowicz and Prahm (1982) for three types of grass vegetation only, making it impossible to adapt the resistance method model to urban situations. Therefore, the surface fluxes of heat, *H*, and water vapor, *LE*, were calculated by incorporating the scheme of Holtslag and van Ulden (1983). Their scheme, following the Penman-Monteith approach (Monteith 1981), also depends on two empirical parameters, α and β'; the sensible heat flux is parameterized as

$$H = \frac{(1-\alpha)+\gamma/s}{1+\gamma/s}\left(Q^* - G\right) - \alpha\beta' \tag{1}$$

and the latent heat flux by

$$LE = \alpha\left(\frac{1}{1+\gamma/s}\left(Q^* - G\right) + \beta'\right) \tag{2}$$

where Q^* denotes the net radiation, G the ground heat flux, $s = \partial q_s/\partial T$, q_s the saturation specific humidity; $\gamma = C_p/\lambda$, C_p is the specific heat of air at constant pressure, and λ the latent heat of water vaporization.

The value of α can be computed from observations; it depends on the surface moisture condition. For bare soil, $\alpha = 0$, so that $LE = 0$. For the Prairie Grass experiment, $\alpha = 0.45$ (Holtslag and van Ulden 1983). For vegetated surfaces with enough water to evaporate, $\alpha = 1$. Because of the reduced water storage capacity and the fast run-off, the following parameterization has been introduced into OML's preprocessor for use over urban surfaces:

$$\alpha = \begin{cases} 1 & \text{hours with rain reported} \\ 0.45 & \text{first hour after rainfall} \\ 0.2 & \text{accumulated net radiation} < 300\ \text{Wh}\cdot\text{m}^{-2} \\ 0 & \text{otherwise} \end{cases} \tag{3}$$

The accumulated net radiation is calculated as the sum of the net radiation for each hour since rain fall stopped. With Eq. (3), the parameter α is not a constant anymore, and the urban energy budget becomes a function of the accumulated net radiation.

The net radiation (Eqs. 1 and 2) is calculated with OML's routine which is based on the scheme of Nielsen *et al*. (1981). For daytime hours, this scheme calculates Q^* as a function of the global radiation; for nighttime hours, Q^* is a function of the difference between incoming and outgoing radiation, cloud cover and albedo. Transition of night- to daytime hours and vice versa is defined by the sign change of the solar elevation angle. The albedo is set to 0.16 (Oke 1988). For snow covered surfaces, the albedo ranges from 0.95 for fresh snow to 0.40 for old snow (Stull 1998, p. 258; Oke 1987, p. 12). In this study, 0.60 has been chosen as averaged snow albedo value, reflecting the fact that within cities, the snow normally is removed from major streets almost immediately, and gets dirty soon.

The ground heat flux G (Eqs. (1) and (2)) is parameterized as a function of the net radiation. Oke and Cleugh (1987) derived the following expression for a suburban area:

$$G = \begin{cases} 0.25\left(Q^* - 27\,\mathrm{Wm^{-2}}\right) & \text{(daytime)} \\ 0.67Q^* & \text{(nighttime)} \end{cases} \tag{4}$$

Irregularly spaced, large roughness elements affect the stability regime. Such elements cause additional mechanical turbulence. This leads to a tendency for the atmospheric night-time stability towards neutral conditions, when compared to the rural areas surrounding the city. During day-time, the same roughness elements counteract the development of large convective eddies as well as a pronounced negative potential temperature gradient. This causes a trend of the day-time stability regime towards neutral conditions as well.

The default minimum value of the Obukhov length within the OML preprocessor is $100z_0$, i.e. roughly equal to ten times the average obstacle height. For cities with a roughness length of order 1 m, this leads to a minimum value of L of 100 m. Hanna and Chang (1992; 1993) use minimum L values over urban terrain as well, being a function of the height of the roughness elements, h. For the present work, OML's minimum value has been applied to unstable atmospheric stability as well, i. e.,

$$\left|L\right|_{\min} = 100z_0 \tag{5}$$

In addition, the minimum value of the friction velocity, which has an original minimum value of $0.001\,\mathrm{ms^{-1}}$ within the OML, has been raised to $u_{*,\min} = 0.1\,\mathrm{ms^{-1}}$ for urban areas.

7.2.4 Modification of the dispersion model

Plume rise plays an important role in determining surface concentrations for real sources. Within cities, almost all emissions originate from combustion processes (road traffic, domestic heating, waste incineration, etc.) and thus have a buoyancy induced plume rise. On the aggregated level of gridded emission inventories, the individual characteristics of stacks (like diameter, temperature excess, and vertical exit velocity) are of no importance. But the over-all effect of plume rise should be parameterized and included in the model.

Within the OML, the commonly used plume rise schemes of Briggs (1984) are implemented, which express the final rise height of the buoyant release as a function of, among other parameters, the buoyancy flux, the mean wind speed at the stack tip, and the friction velocity. For the present purpose, these schemes are translated for use in connection with domestic heating and traffic area sources by choosing average stack heights above roof level and above the street level, respectively. Instead of specifying values for vertical exit velocity and source radius, averaged buoyancy fluxes are assigned to the individual sources depending on the source strength (being a function of time and of space). The temperature of the emissions is set to a constant level and not to a constant excess with respect to the ambient temperature. This has been done in order to reflect the more or less constant burning temperature of engine vehicles and of heating.

The well known Gaussian plume solution to atmospheric dispersion does not apply close to the source, since all parameterizations of the vertical and lateral plume standard deviation, $\sigma_y(x)$ and $\sigma_z(x)$, respectively, approach zero near the source. This causes the ground level concentration prediction of Gaussian plume models to approach infinity for $x \to 0$, since both $\sigma_y(x)$ and $\sigma_z(x)$ appear in the denominator of an exponential expression. The minimum source-receptor distance depends on the difference between release and receptor height as well. For example, Briggs (1973) mentions $x > 100\,\mathrm{m}$ as the range of applicability of the Gaussian plume equation. Therefore, many applied Gaussian plume models either impose a lower limit on $\sigma_y(x)$ and $\sigma_z(x)$, or an upper limit on the near-source concentration.

When using Gaussian plume models together with gridded emission inventories of a finer scale, the Gaussian plume expression has to be replaced by another model for the near-source field, in fact yielding a hybrid dispersion model. Otherwise, small sources, which are located in the vicinity of any receptor in an urban environment, may promote an average (potentially large) overestimation of concentration.

Within the OML dispersion model, there is no special near-source dispersion model for point sources, but for area sources, a lower limit of half the horizontal extension of the area source applies to $\sigma_y(x)$ and $\sigma_z(x)$. This effectively prevents the near-source concentration from going to infinity. However, the OML scheme yields a different lower limit to $\sigma_y(x)$ and $\sigma_z(x)$ when, for example, a 100 m x 100 m area source is numerically replaced by four 50 m x 50 m sources with one fourth the original emission rate each.

Therefore, in the present study, the ground level concentration prediction is subject to an upper boundary

$$C_{\max} = \frac{Q}{\Delta x \Delta y \overline{U}} \tag{6}$$

Here, $\overline{U}$ denotes the average mean wind speed representative for the area source, as used in the well-known Gaussian dispersion equation. Equation (6) means that the concentration within the area of the source is set equal to the concentration which would be in place within an ”infinite” area source, with source strength Q (in units g·s^{-1}) per area of size $\Delta x \times \Delta y$, regardless of atmospheric stability.

Although Eq. (6) does not explicitly take into account the boundary of the area source (Eq. 6 being applied to all distances down-wind from the source), the transition is smooth and takes places in the proximity of the boundary of the area source. Figure 2 shows a comparison between the original OML area source near-field scheme, and Eq. (6). As can be seen, Eq. (6) yields the identical upper concentration limit, since it depends on the normalized emission rate. The original OML scheme, on the other hand, is an explicit function of the source size, and thus yields different results when the resolution of an emission inventory is changed from, for example, a 1 km grid to a 100 m grid.

7.3 ZURICH 1990 CASE STUDY

7.3.1 Zurich 1990

The city of Zurich has approx. 370 000 inhabitants and covers an area of 88 km^2. This area consists of 4226 ha natural surface (forests, parks, agricultural areas, cemeteries, water) and 4548 ha covered surface (buildings, roads, infrastructure, industry). Figure 3 depicts the land use of the city of Zurich aggregated into six main categories.

Data from a meteorological station from the national weather service are available which is situated within the city. This station covers all ground observations needed. As an example, the wind rose for the entire year 1990 is depicted in Figure 4. For the determination of the mixing height, the OML preprocessor requires vertical profiles of temperature and density. For this, the radio soundings (twice daily) from the Payerne station, 200 km away from Zurich, have been used. The Payerne site is the only meteorological station in Switzerland conducting radio soundings.

7.3.2 Classification of concentration measurement locations

For the year of 1990, a total of 28 stations spread all over the city, yielded observational data of surface pollutant concentrations for comparison to the simulations. Besides from 4 continuously monitoring stations (hourly averaged concentrations for the whole year), pollutant concentrations were measured at the remaining 24 stations during 40 to 45 periods of 24 hours each (covering all seasons, and all days of the week), from the results of which annual averaged concentrations were estimated. Figure 5 shows the position of the air pollution monitoring stations from which data have been used for model validation in the present study.

Due to the use of gridded emission inventories, we are able to predict area averaged concentrations only. The measured concentrations, however, will essentially be point concentrations. These point concentrations may be influenced by local emission sources (like major roads), or they may not (yielding the urban background concentration). If local influences are present, they may either be resolved by the emission inventory, or they may not.

The representativeness of measurement stations depends on the local influence from roads or near-by buildings. In the present study, the model performance validation is

done separately for three groups, as defined in Table 1 (urban background, influenced by major roads with or without local influences). To determine the specific group, all measurement sites have been investigated in detail.

To describe the immediate and local environment of each measurement site, the surroundings have been identified from maps, and the locations were visited in the field where necessary. The details of the environment description scheme used are given in Table 2. Table 3 gives some additional details on the concentration monitoring sites, along with the coordinates as depicted in Figure 5. The boundary for the so-called "immediate" environment has strictly been set to 100 m, that of the "local" environment to 1 km. For stations situated near major roads, the daily traffic volume is given as well. The resulting station classification in the groups Q1, Q2 and Q3, respectively, as adopted in this study (listed in Table 3), is mainly influenced by the "immediate" environment.

Any dispersion model would be expected to perform best in predicting the urban background (Q1 data in this study), second-best in predicting concentrations where roads are adequately resolved in the emission inventory (Q2), and to show considerable error when local effects are present on scales smaller than the spatial concentration sampling scale (Q3).

When a concentration measuring unit is positioned such that strong local influences exist (for example in a street canyon), the measured concentration may strongly depend, for example, on the mean wind direction. Then, the stationarity condition, and the ensemble-average approach, only allow for concentration sampling times of 24 hours and longer to be compared with the corresponding model predictions. They also do not allow for the comparison of the distribution of hourly concentration, i.e. of quantile-quantile plots of predicted vs. observed concentration, as a model validation tool for such sites with local influences.

7.3.3 Emission inventory

The emission rate of a single large source can easily be measured, but estimating the total emissions of an agglomeration is more difficult. Uncertainties exist on the emission level of road traffic as well as the traffic volume itself, on the emission level for the various other fossil burning processes, etc. Although no dispersion model prediction can

be more accurate than the emission inventory it relies upon, these inherent uncertainties of urban emission inventories are not addressed here. The focus is on the modeling of dispersion.

For the city of Zurich in the year 1990, a detailed (100 m x 100 m resolution) emission inventory was constructed (Werfeli 1995). It takes into account traffic (number of vehicles per day and estimated speed on the 152 largest roads of the city; additionally, estimates of short-distance traffic not using major roads), domestic and commercial heating and the 33 largest industrial sources (treated as point sources in the model).

This emission inventory sums up to over 4300 SO_2 sources and over 4300 NO_x sources, where the line sources (roads) are split up and added to area sources. To simulate the time dependence of source strength, the amplitude of the traffic sources is modulated according to the hour of the day and the day of the week, and the strength of the heating sources depends on the hour of the day and on the month. Among the observational data, traffic frequency data at four sites within the city are available, which have been used to construct average hourly and daily frequency cycles.

The emission data of the heating sources was collected very carefully and the traffic emissions were modeled using numerous results from actual traffic census data. The emission factors used for the calculation of the overall emissions for each source type and pollutant were checked with in-site monitoring measurements. With this procedures the overall accuracy of the emission data is estimated at ±5% for heating sources (SO_2 and NO_x) and at ±20% for NO_x and ±25% for SO_2 for emissions from traffic sources. This amounts to a total maximum estimated error in the emission data of 6.3% for SO_2 and, due to the larger contribution of traffic sources, of 14.3% for NO_x.

7.3.4 Urban set-up

The definition of the model surface is another key factor in the appropriate model set-up. When adapting continuous plume models to urban environments, there is no such thing as an averaged mean wind speed in the lowest, say, ten meters, i.e. between the building structures themselves. In order to avoid the use of a (relatively simple) Gaussian model for dispersion estimates *between* the roughness elements, a model surface corresponding to the zero displacement height (see Rotach 1994) rather than the physical surface $(z = 0)$ has been chosen. For the city of Zurich, the average building

height is h = 12 m (Rotach 1995); the thickness of the RS has been chosen to be 3h. This corresponds with the approach adopted by Hanna and Chang (1993), where the depth of the mechanically well-mixed layer is set at three times the average obstacle height.

The zero displacement height, d, is set at 0.75h (Rotach 1994), as sketched in Figure 6. The height of the domestic and industrial area sources has been set to 5 m above the average building height, reflecting the fact that chimneys are situated at the very top of every building, and that in general stacks with emission rates above average are to be found on buildings with a height above average. The emission height of the traffic area sources corresponds to the lower model boundary. For the 33 largest sources, which are treated as individual point sources within this simulation, the emissions take place at the physical stack height. All concentrations have been predicted for a receptor height of $z' = 0\,\mathrm{m}$, where $z' = z - d$, i.e. at the lower model boundary.

No attempt has been made to develop vertical profiles of concentration within street canyons, in order to extrapolate any concentrations predicted at the $z' = 0\,\mathrm{m}$ level down to the physical ground level. In general, concentrations at street level are higher than at a height of several meters, i.e. $z' = 0\,\mathrm{m}$ (e.g. Lee and Park 1994; Zoumakis 1995). The measurements took place at 2 m above ground level, i.e. well below $z' = 0\,\mathrm{m}$ (for some of the continuously measuring stations, the receptor height is 5 m). But as the emission inventory does not resolve single street canyons, and since such influences depend on the wind direction and the surrounding buildings, such an extrapolation cannot be expected to improve the model accuracy. Instead, we will (in section 7.4) evaluate the predicted concentrations for the stations groups Q1 to Q3 separately. It is assumed that street canyon effects only occur at Q3 sites.

Special care has been taken to estimate the buoyant plume rise of the emissions. The buoyancy flux, $F_B = g\, F_V\, \Delta T/T_a$, is determined by the estimated maximum volume flux (as summarized in Table 4), F_V, caused by domestic heating. The maximum volume flux from Table 4 applies to daytime conditions during the coldest day of 1990 only: The actual volume flux is time dependent, where the same time series of scaling factors has been used as for the emission rate of the domestic area sources themselves (see preceding section). The temperature of the emission itself does in general not depend on

the ambient temperature; it is determined by the technical lay-out of the heating equipment. Therefore a constant level of exhaust gas temperature has been chosen.

The exhaust gases from mobile sources will experience a buoyancy induced rise as well. Here, we only address the over-all rise of traffic area source emissions, not of individual vehicles. Given the thermodynamical effectiveness of below 40% for gasoline engines, a considerable amount of heat is released through the tail pipe. But the exact proportion of energy being radiated as heat, emitted through the tail pipe, or being used for chemical reactions in the catalytic converters, is unknown. In general, the exhaust gas temperature does depend on the previous minutes of driving behavior of the vehicle. In congested (stop-and-go) traffic conditions, the catalytic converter is likely not to reach the required temperature level, causing the emission level to increase drastically as compared to fluent traffic conditions. Nevertheless the resulting buoyancy of traffic area sources has been scaled with the time series of traffic volume (see preceding section).

7.3.5 Background concentration

Even the “perfect” dispersion model and emission inventory should under-predict the observed concentrations by the amount of the natural, regional background. An estimate of this natural background is difficult to obtain in the case of the city of Zurich, because such locations, where one can be sure that there is no influence of local anthropogenic emissions, are to be found at high altitudes in the Swiss mountains only. Additionally, there is the impact of all the sources situated in the vicinity of the city, but which are not covered by the city’s emission inventory. Hence, what is needed as “background” concentration is the sum of the natural background and of the (yearly averaged) concentration impact from all the sources that are in the agglomeration around the city (i.e. not part of the modeling domain). Therefore the “background” concentration cannot be a single constant level, but will be spatially varying, with lowest values in the center of the domain, increasing towards the boundaries of the emission inventory.

In order to obtain such a city background concentration map, the results from another study have been used where yearly averaged NO_2 concentrations have been computed for whole Switzerland (SAEFL 1997). For the present study, a special concentration map has been computed based on the emission inventory of the state of Zurich, where all those sources which are situated within the city itself have been removed. This yields

the complementary concentration map to the present work. Although the SAEFL (1997) dispersion model is simplified, and is not able to take into account the urban characteristics of the area, the results are considered to be accurate enough for use as a background concentration map.

Several steps are needed to transform the results into the required background concentration map. The underlying emission inventory in SAEFL (1997) is for NO_x, which is transformed into NO_2 with an exponential relationship which has been fitted to observations. The inverse function is thus applied to obtain the underlying NO_x concentrations needed for this study. The SAEFL (1997) concentrations are predicted as the sum of a regional (including the natural and non-Swiss contributions) and a national (anthropogenic) background, and a contribution from local sources. The background concentrations, which are based on a 1995 emission inventory, are transformed into values for 1990 by re-scaling the national component by the ratio of the 1990 to 1995 total NO_x emissions of Switzerland taken from SAEFL (1995).

SAEFL (1997) assumes an exponential decrease of the background concentration with increasing height above sea level. This causes very high background values for lower altitudes. This is partly caused by the fact that long-range (distances > 2 km) dispersion is not implemented in the SAEFL (1997) dispersion model. This causes a missing contribution to the local concentrations. By fitting the model predictions to observations, the exponential relationship has come to account for this in the SAEFL (1997) model. For the purpose of the present work, this exponential relationship has been replaced by a linear regression expression, which has itself been fitted to measurements of approximate background concentration.

The SO_2 background map has been derived from the NO_x background by a straight-forward procedure. For the four stations with hourly observed concentration, the NO_x-to-SO_2-ratio of the average of the 876 hours (i.e. 10% of the year) with the lowest observed concentrations has been computed (see Table 5). This ratio differs, depending on the quality of the measurement station. For the true urban background (Q1 station), this ratio is higher as compared to the site with some local influences (Q2), and much higher for data obtained from sites exposed to streets (Q3). For the present purpose of a background map, the NO_x background concentration has been divided by the ratio of

18.7 from the true urban background station. The resulting NO_x and SO_2 background maps are shown in Figure 7.

7.4 RESULTS

7.4.1 Overview

The OML has been used to predict SO_2 and NO_x concentrations at a uniform receptor height (located at the zero plane displacement height) at the positions of the 28 observational stations and at a regular grid covering the whole modeling domain with a spacing of 1000 m. The simulation has been run for the whole year 1990, with a principal time step of one hour.

Two different simulation runs have been conducted:

- 'non-urban' simulation: application of the OML model 'as it is', with the set-up as shown in Figure 6, roughness length $z_0 = 1$ m, area source plume rise settings as outlined in section 7.3.4, and the near-source concentration limit according to Eq. (6).
- 'urban' simulation: application of the 'OML-Urban' model, i.e. the OML with the modifications from section 7.2.3 (urban energy balance in meteorological pre-processor, Eqs. (1) to (5)) and section 7.2.4 (local scaling with friction velocity as a function of height). All other settings are identical to the 'non-urban' simulation run.

The major goal of the investigation is the correct prediction of the annual average concentration. New generation type Gaussian plume models are generally accepted to be suited for such predictions. However, a wide range of assumptions regarding source characteristics has inevitably to be made, as has been outlined in the previous sections. To minimize the risk that the correct annual average prediction (as it can be verified with respect to the 28 observational stations) actually arises from the sum of various severe over- and underpredictions, caused by inadequate parameterizations and/or source specifications, a multi-step validation procedure is undergone.

First, we will assess the effect of those parameters for which actual "urban" values have been chosen. Secondly, we will compare the hourly predicted concentration time series to the observed daily cycles of continuous (i.e., hourly) observations. Third, using

quantile-quantile plots it can be verified whether the distribution of predicted concentrations resembles the observed distribution. This is done for the 8760 hours of observations at the four continuously measuring stations. Finally, we will calculate the performance statistics of the predicted annual mean concentration at the positions of the 28 observational stations, separate for each receptor "quality group".

7.4.2 Pollutants considered

NO_2 is one of those pollutants which frequently exceeds the threshold value of the Swiss clean air act. The permitted yearly average is 30 µg m^{-3} for NO_2; the threshold of 80 µg NO_2 m^{-3} may be exceeded only once per year based on a 24-hour average, and the threshold of 100 µg NO_2 m^{-3} must not be exceeded during 95% of all 30-minute averages over the whole year. These limit values are considerably lower than in most other countries, including the United States. The chemical conversion of stack and tail pipe NO emissions to NO_2 takes place over distances of some hundred meters. Therefore, in this study, NO_x rather than NO_2 is modeled, which is a more robust quantity.

On the side of the emission inventory, the NO_x emissions consist of the sum of the two components NO and NO_2. On the side of the measurements from the air pollution monitoring stations, again the sum of NO and NO_2 is used for NO_x. The assumption that NO_x can be assumed as a tracer quantity holds to a high degree.

The other pollutant considered in the present study is sulfur dioxide (SO_2). Due to a general tendency of decreasing concentrations, the importance of this pollutant as a risk factor to human health is decreasing. The corresponding annual average threshold (30 µg m^{-3}) of the Swiss clean air act is not violated anymore in the city of Zurich at present. This is mainly due to the use of low-sulfur oil for domestic as well as commercial heating purposes. Also, the 100 µg m^{-3} threshold, which may be exceeded during only 1 day per year and during only 5% of all 30-minute averages as well, is not violated any more at present. SO_2 has been included in this study because unlike NO_x, which is emitted mainly by road traffic at street level, SO_2 originates for the larger part from residential and commercial non-mobile sources with different source characteristics.

7.4.3 Main effects of urban modification

A number of runs were performed with the OML using various configurations in connection to the points mentioned above, to find an optimal set-up for an urban dispersion simulation. Only when such a set-up is identified, it makes sense to introduce the roughness sublayer effects in order to (i) increase the physical significance of the dispersion simulations and (ii) see whether this additional change is likely to improve the quality of the simulation.

In this section, we investigate the effect of the most important ”urban” settings. The parameter with the largest influence on the ability to predict hourly concentrations is the roughness length z_0, because of the lower limit on the absolute value of Obukhov length, L (Eq. (5)). A histogram of the Obukhov length is displayed in Figure 8. More than 53% of all hours of the year are affected by this limit (note that the $100\,z_0$ limit is part of the standard OML meteorological pre-processor, and has not been changed for the present study).

The second-largest impact on the meteorological scaling parameters is caused by the increased lower limit to the friction velocity adopted in this study (section 7.2.3). In 18% of all hours of the year, the friction velocity equals this minimum value (Figure 9).

The simulation for the city of Zurich for the year 1990, of which the results are discussed in the next sections, has also been performed with a ‘semi-urban’ approach, i. e. by only introducing the RS turbulence but without the urban modifications to the energy balance as discussed in section 7.2.3 (affecting the albedo, the snow albedo, the ratio of sensible to latent heat flux, and the moisture availability). The combined effect of these urban energy balance settings alone is a decrease in NO_x annual averaged concentrations of 0.17%, and of 1.8% for SO_2. Since the major part of domestic emissions (which dominates the SO_2 concentrations) is emitted during winter conditions, the larger effect on SO_2 concentrations is likely to be caused in large part by the change in snow albedo.

7.4.4 Hourly predictions, reproduction of frequency distribution

Figure 10 shows an example of the hourly observed and predicted (both ‘non-urban’ and ‘urban’ approaches) NO_x concentrations. The daily cycle with concentration peaks induced by the road traffic peak hours can be clearly seen (the station depicted is a Q2

station with some influence from local traffic, but not located directly near a road) as well as the much lower concentration level on Sep. 16 (a Sunday).

Gaussian models with gridded emission inventories can not be expected to yield close hour-to-hour correspondences. This would need careful modeling of the actual flow field at each receptor site, and the use of a very fine emission inventory with individual source heights. But Figure 10 shows that there is neither a general underprediction nor overprediction during certain hours of the day: the night-time concentration level is well predicted, and the height of the concentration peaks during day-time always is of similar magnitude. This is to a large part due to the lower limit to the absolute value of the Obukhov length (Eq. 5). Without this limit, which would neglect the important role of mechanically induced turbulence by the buildings, a severe underprediction during night and corresponding overprediction during the day would result.

The differences between "urban" and "non-urban" approach are not very pronounced during night-time hours. During day-time conditions, however, the peak concentration generally is clearly higher for the "urban" approach.

Figure 11 depicts the so-called quantile-quantile plot for one out of the four stations with continuous measurements. For both the "urban" and "non-urban" set-up the graph is almost a straight line, indicating that the frequency distribution of predicted low and of high concentrations corresponds very well to observations. The "urban" simulation leads to a general increase of predicted concentrations of 35%.

7.4.5 Annual averages, statistical performance

A scatter plot with the annual averaged NO_x and SO_2 concentration is depicted in Figure 12. The different monitoring site groups Q1 to Q3 are marked with different symbols; additionally, large symbols denote stations with continuous measurements. For all stations, both the "urban" and "non-urban" simulation results are shown (filled and open symbols, respectively). In Table 6 the following statistical measures are compared for the two different simulations:

FB	the fractional bias: $FB = (\overline{C}_{\text{obs.}} - \overline{C}_{\text{pred.}}) \big/ (0.5(\overline{C}_{\text{obs.}} + \overline{C}_{\text{pred.}}))$
NMSE	the normalized mean square error: $NMSE = \overline{(C_{\text{obs.}} - C_{\text{pred.}})^2} \big/ (\overline{C}_{\text{obs.}}\overline{C}_{\text{pred.}})$
COR	the correlation coefficient: $COR = \overline{(C_{\text{obs.}} - \overline{C}_{\text{obs.}})(C_{\text{pred.}} - \overline{C}_{\text{pred.}})} \big/ (\sigma_{\text{obs.}}\sigma_{\text{pred.}})$
FAC2	percentage of simulations within a factor of two of the measurement

Here, $C_{obs.}$ is the observed concentration and $C_{pred.}$ the predicted one.

The performance of the OML-Urban model, with FAC2 = 100% for NO_x and SO_2 for Q1 and Q2 stations, is considered to be very satisfactory, showing that Gaussian plume models may be applied to urban environments, when some corrections are made, for the prediction of yearly averaged concentration. As expected (Section 7.3.2), the model performance is best for Q1 monitoring stations, second-best for Q2 data, whereas for Q3 locations, the local influence of major roads (not fully resolved by the gridded emission inventory) causes a slight underprediction of ground-level concentrations. All Q1 and Q2 data for both NO_x and SO_2 are within a factor of 2 from the observed values.

The bootstrap resampling method proposed by Hanna (1989) together with percentile-based resampled confidence intervals of 95% has been used to assess the presence of systematic errors. The NO_x predictions are almost bias-free, the FB value of 0.042 and 0.033 for Q1 and Q2 sites, respectively, not being significantly different from zero. Also, the FB value of 0.026 for Q1 stations for SO_2 does not differ significantly from zero, but it does for Q2 data. Figure 12 also confirms that whereas for NO_x, the 'urban' approach leads to an essentially bias-free prediction, for SO_2 the underprediction for the 'non-urban' approach turns into a slight overprediction when using the 'urban' set-up. Especially, the annual average concentration observed at the two continuously measuring stations being classified as Q1 or Q2, is very closely reproduced for NO_x. For SO_2 a small systematic overprediction of concentrations persists.

Table 7 gives the relationship between domestic/industrial and traffic area source emissions on the one hand, and the share of the respective source categories on the predicted ground-level (at the lower model boundary, i.e. z = 9 m) concentration on the other hand. The combined effect of the higher emission height and of the more pronounced buoyancy of the domestic/industrial emissions causes a decrease in the contribution to the concentration impact, as compared to the share in the emissions. For example, although over 38% of all NO_x emissions originate from non-mobile sources, the street-level concentrations (when the arithmetic mean over all station locations is computed) are influenced by the traffic emissions by more than 88% (without the background concentration).

7.5 SUMMARY AND CONCLUSIONS

To obtain a proper modification of operational (Gaussian) dispersion models for use within an urban environment, the concept of an "urban preprocessor" (Rotach 1997a) has been introduced. Its basic principle is to use similarity theory based on local fluxes for the parameterization of the turbulence structure within the urban roughness sublayer. The first validation step of this concept has been reported on elsewhere (Rotach and de Haan 1997) and was performed by use of a Lagrangian particle dispersion model for the simulation of a (sub)urban tracer experiment. A clear improvement of the predictability was the result. This indicates that the urban preprocessor is able to better take into account the rough character of the surface at the sites where this experiments took place. As a second validation step the performance of the operational Gaussian multi-source dispersion model OML for this experiment (Copenhagen) as well as for Lillestrøm showed a similar improvement of the correspondence between the simulated and the measured concentrations, when introducing the roughness sublayer (de Haan *et al.*1998). Therefore, the concept of the urban preprocessor can be used with operational Gaussian dispersion models to improve the model's prediction skills over urban surfaces.

The resulting OML-Urban model is used for the case study of the yearly average surface pollution concentration (NO_x and SO_2) in the city of Zurich in 1990, for which a very detailed emission inventory (100 m x 100 m resolution) is available. Some parameterizations within OML's meteorological pre-processor were changed in accordance with an urban energy budget. Data from air pollution monitoring stations were grouped according to the influence of nearby roads. The performance of OML-Urban is assessed for these different groups separately. The resulting prediction skill is very satisfactory, with a close reproduction of the frequency distribution of observed concentration, all predictions being within a factor of 2 of the observed values, and a small systematic error (bias). It is concluded that the method presented is suitable to allow the application of Gaussian plume models to urban environments for the prediction of yearly averaged concentrations.

Acknowledgements—The comments and suggestions of Dr S. R. Hanna and of Dr H. R. Olesen have been very helpful. Thanks go to Dr J. Heldstab and Dr T. Künzle for providing the background NO_x concentration map for the city of Zurich. The present work was partly financed by the Swiss Agency of Education and Sciences (BBW) through the TMR network (TRAPOS), and by the Swiss National Science Foundation through Grant No 21-46849.96.

REFERENCES

Berkowicz, R., and Prahm, L. P. (1982): Sensible heat flux estimated from routine meteorological data by the resistance method. *J. Appl. Meteor*., **21**, 1845–1864

Briggs, G. A. (1973): Diffusion estimation for small emissions. 1973 Annual Report, Air Resources Atmos. Turb. and Diffusion Lab., Environmental Lab., Report ATDL-106, USDOC-NOAA

Briggs, G. A. (1984): Plume rise and buoyancy effects. Atmospheric Science and Power Production (ed. by Randerson D.), DOE/TIC 27601. Department of Commerce, Springfield, USA

Carruthers, D. J., Holroyd, R. J., Hunt, J. C. R., Weng, W.-S., Robins, A. G., Apsley, D. D., Smith, F. B., Thomson, D. J. and Hudson, B. (1992): UK Atmospheric Dispersion Modelling System. In: van Dop, H. and Kallos, G. (eds.), *Air Pollution Modelling and its Applications IX*, Plenum Press, New York

Feigenwinter, C.; Vogt, R. and Parlow, E. (1998): Vertical structure of selected turbulence characteristics above an urban canopy. Accepted for publication in *Theor. Appl. Clim.*

Gryning, S.-E., and Lyck, E. (1984): Atmospheric dispersion from elevated sources in an urban area: Comparisons between tracer experiments and model calculations. *J. Clim. Appl. Meteorol*., **23**, 651–660

de Haan, P., Rotach, M. W, and Werfeli, M. (1998): Extension of an operational short-range dispersion model for applications in an urban environment. *Int. J. Vehicle Design*, **20**, 105–114

Häggkvist, K. (1997): Evaluation of dispersion models for an urban environment, an example from Stockholm, Sweden. *Inter. J. Environment Pollution*, **8**

Hanna, S. R. (1989): Confidence limits for air quality model evaluations, as estimated by bootstrap and jackknife resampling methods. *Atmospheric Env.*, **23**, 1385–1398

Hanna, S. R. and Chang, J. C. (1992): Applied dispersion modeling over urban areas. *Bound. Layer Meteor.*, **58**, 229–259

Hanna, S. R. and Chang, J. C. (1993): Hybrid Plume Dispersion Model (HPDM) improvements and testing at three field sites. *Atmospheric Env.*, **27A**, 1491–1508

Härkönen, J., Kukkonen, J., Valkonen, E., and Karppinen A. (1998): The influence of vehicle emission characteristics and meteorological conditions on urban NO_2 concentrations. *Int. J. Vehicle Design*, **20**, 125–130

Haugsbakk, I., and Tønnesen, D. A. (1989): Atmospheric dispersion experiments at Lillestrøm 1986–1987. Data Report NILU OR 41/89. Available from Norwegian Inst. for Air Research, PO Box 100, N-2007 Kjeller, Norway

Högström, U., Bergström, H., and Alexandersson, H. (1982): Turbulence characteristics in a near-neutrally stratified urban atmosphere. *Boundary-Layer Meteorol.*, **23**, 449–472

Holtslag, A. A. M., and van Ulden, A. P. (1983): A simple scheme for daytime estimates of the surface fluxes from routine weather data. *J. Clim. Appl. Meteor*., **22**, 517–529

Lee, I. Y. and Park, H. M. (1994): Parametrization of the pollutant transport and dispersion in urban street canyons. *Atm. Environment*, **28**, 2324–2349

Monteith, J. L. (1981): Evaporation and surface temperature. *Quart. J. Roy. Meteorol. Soc.*, **87**, 159–170

Oikawa, S., and Meng, Y. (1995): Turbulence characteristics and organized motion in a suburban roughness sublayer. *Boundary-Layer Meteorol.*, **74**, 289–312

Oke, T. R. (1987): Boundary layer climates. 2nd edition. Methuen, London

Oke, T. R. (1988): The urban energy balance. *Progress in Physical Geography*, **12**, No. 4, 471–508

Oke, T. R., and Cleugh, H. A. (1987): Urban heat storage derived as energy balance residuals. *Boundary-Layer Meteorol.*, **39**, 233–245

Olesen, H. R., and Brown, N: The OML meteorological preprocessor; a software package for the preparation of meteorological data for dispersion models. MST Luft-A 122, 2nd ed. To be obtained from National Environmental Research Institute, DK-4000 Roskilde, Denmark

Olesen, H. R., Løfstrøm P., Berkowicz R. and Jensen A. B. (1992): An improved dispersion model for regulatory use: the OML model. In van Dop H. and Kallos G. (eds.), Air Pollution Modeling and its Applications IX, Plenum Press, New York

Olesen, H. R. (1995): The model validation exercise at Mol: Overview of results. *Int. J. Environment Pollution*, **5**, 761–784

Rafailidis, S. (1997): Influence of building areal density and roof shape on the wind characteristics above a town. *Boundary-Layer Meteorol.*, **85**, 255–271

Raupach, M. R., Antonia R. A. and Rajagopalan S. (1991): Rough-wall turbulent boundary layers. *Appl. Mech. Rev.*, **44**, 1–25

Rotach, M. W. (1993a): Turbulence close to a rough urban surface. Part I: Reynolds stress. *Boundary-Layer Meteorol.*, **65**, 1–28

Rotach, M. W. (1993b): Turbulence Close to a Rough Urban Surface Part II: Variances and Gradients. *Boundary-Layer Meteorol.*, **66**, 75–92

Rotach, M. W. (1994). Determination of the zero plane displacement in an urban environment. *Boundary-Layer Meteorol.*, **67**, 187–193

Rotach, M. W. (1995). Profiles of turbulence statistics in and above an urban street canyon. *Atm. Environment*, **29**, 1473–1486

Rotach, M. W., Gryning, S.-E. and Tassone, C. (1996): A two-dimensional stochastic Lagrangian dispersion model for daytime conditions. *Quart. J. Roy. Meteorol. Soc.*, **122**, 367–389

Rotach, M. W. (1997a): Towards meteorological preprocessing for dispersion models in an urban environment. *Inter. J. Environment Pollution*, **8**, 548–556

Rotach, M. W. (1997b): The turbulence structure in an urban roughness sublayer, in: Perkins, R. J. and Belcher, S. E. (Eds): Flow and dispersion through groups of obstacles, Clarendon Press, Oxford, 143–155

Rotach, M. W., and de Haan, P. (1997): On the urban aspect of the Copenhagen data set. *Inter. J. Environment Pollution*, **8**, 279–286

Roth, M., and Oke, T. R. (1993): Turbulent transfer relationships over an urban surface. I: Spectral characteristics. *Quart. J. Roy. Meteorol. Soc.*, **119**, 1071–1104

Roth, M. (1993): Turbulent transfer relationships over an urban surface. II: Integral statistics. *Quart. J. Roy. Meteorol. Soc.*, **119**, 1105–1120

SAEFL (1995): Anthropogenic emissions of air pollution in Switzerland from 1900 to 2010. (in German or French, with English abstract). Swiss Agency for Environment, Forests and Landscape, SRU No 256, Berne, Switzerland

SAEFL (1997): NO_2 concentration in Switzerland 1990 to 2010 (in German or French; with English abstract). Swiss Agency for Environment, Forests and Landscape, SRU No 289, Berne, Switzerland

Stull, R. B (1988): An introduction to boundary layer meteorology. Kluwer Academic Publishers, Dordrecht, the Netherlands

Werfeli, M. (1995): Modelling surface pollutant concentrations (SO2 and NOx) in the city of Zurich. *Inter. J. Environment Pollution*, **5**, 575–584

Zilitinkevich, S. (1972): Determining the height of the nocturnal boundary layer. *J. Appl. Meteorol*., **17**, 28–33

Zoumakis, N. M. (1995): A note on average vertical profiles of vehicular pollutant concentrations in urban street canyons. *Atm. Environment*, **29**, pp. 3719–3725

Table 1: Definition of concentration measurement station quality groups in urban areas.

Group	Description	Examples of locations
Q1	true urban background concentration	Park areas within city, residential areas with very low traffic
Q2	urban background concentration with local influences	Residential areas with non-major roads
Q3	street concentration station	Street canyon, near major roads

Table 2: Description of immediate and local environment of air pollution monitoring stations according to EU Council Directive 92/72/EC on Air Pollution by Ozone.

Immediate Environment (within a radius of 0 to 100 m)	
I1a, I1b, I1c, I1d	large street heavy/medium/local/no traffic
I2a, I2b, I2c, I2d	small street heavy/medium/local/no traffic
I3a, I3b, I3c, I3d	canyon street heavy/medium/local/no traffic
I4	footway
I5	front of building
I6	terrace, tower, belfry
I7	interior court, school, hospital
I8	trees
I9	large flat area
I91	channel
I92	meadow, field
I99	other
Local Environment (within a radius of 100 m to some km)	
LAa, LAb, LAc, LAd	urban commercial/industrial/residential/mixed
LBa, LBb, LBc	industrial heavy/medium/light concentration
LCa, LCb, LCc	road traffic heavy/medium/light
LD	commercial
LE	residential (isolated houses)
LF	harbor
LG	airport
LH	park, forest, natural field
LI	agricultural area
LJ	mountains, valleys
LK	sea side or lake side
LL	other

Table 3: Characteristics and classification of concentration measurement stations in the city of Zurich, 1990 field campaign. Station type "hourly conc." denotes continuos measurements, "annual av." stands for statisically derived annual mean values. For definition of environment description, see **Table 2**. DTV denotes daily traffic volume, "Pop." is population density per ha.

Station name	Type	x-coor-dinate [km]	y-coor-dinate [km]	Immediate environment [<100m]	Local environment [<1km]	DTV [veh./d]	Pop. [inh./ ha]	Noise level [dBA]	Group
Schwamendingen	hourly conc.	684.91	251.43	I7	LAc, LCa		65	55	Q1
Schwamendingen 2	annual av.	684.90	251.45	I7	LAc, LCa		65	55	Q1
Hard	annual av.	680.85	248.60	I7	LAd		91	59	Q1
Seefeld	annual av.	684.40	245.80	I7	LAc		91	60	Q1
Industriequartier	annual av.	682.05	248.80	I7	LAd		134	52	Q1
Oberstrass	annual av.	684.10	248.70	I7	LAc		64	57	Q1
Hirzenbach	annual av.	686.65	250.90	I7	LAc, LCa		84	55	Q1
Sihlfeld	annual av.	680.75	247.60	I8	LAc		n.a.	52	Q1
Enge	annual av.	682.65	245.35	I8, I9	LAc, LK		n.a.	57	Q1
Zoo	annual av.	685.90	248.55	I8, I9	LH		n.a.	47	Q1
Kaserne	hourly conc.	682.43	247.85	I2c, I7	LAd		n.a.	n.a.	Q2
Witikon	annual av.	687.05	245.65	I2c	LE, LH		34	58	Q2
Höngg	annual av.	680.10	250.95	I2c	LE, LH		41	57	Q2
Wollishofen	annual av.	682.20	244.10	I2c	LAc, LCa		47	53	Q2
Leimbach	annual av.	681.40	243.30	I2c	LE, LJ, LCa, LH		30	54	Q2
Altstetten	annual av.	678.55	248.85	I2c	LAc, LH		48	49	Q2
Affoltern	annual av.	680.90	252.45	I2c	LE, LH		37	60	Q2
Seebach	annual av.	683.30	253.35	I2c	LAc, LCa		41	55	Q2
Stampfenbach	hourly conc.	683.14	249.04	I1b, I5	LAd	10 000	84	72	Q3
Stampfenbach 2	annual av.	683.15	249.00	I1b, I5	LAd	10 000	84	72	Q3
Wiedikon	hourly conc.	681.95	247.25	I1a, I3a	LAd	33 000	126	72	Q3
Wiedikon 2	annual av.	681.95	247.25	I1a, I3a	LAd	33 000	126	72	Q3
Bellevue	annual av.	683.55	246.80	I1a	LAa, LK	60 000	38	74	Q3
Friesenberg	annual av.	680.35	246.70	I1a	LE	14 000	42	68	Q3
Wipkingen	annual av.	682.10	249.90	I1a, I3a	LAd	63 000	103	80	Q3
Schörli	annual av.	684.90	251.10	I1a, I3a	LAc, LH	83 000	65	75	Q3
Oerlikon	annual av.	683.40	251.40	I3a	LAd	18 000	62	70	Q3
Hirslanden	annual av.	685.00	246.10	I3b, I1b	LAc	15 000	74	72	Q3

Table 4: Assumptions for the estimation of buoyant rise of area source (heating and traffic) emissions. The max. buoyancy flux is multiplied with a monthly, daily and hourly varying time series to obtain the appropriate buoyancy flux for each season (heating) or time of day (traffic).

	domestic and commercial area sources	**traffic area sources**
max. volume flux per household	18 m^3 / h / household	
av. number of households per building	7.5	
max. volume flux per source	120 m^3 / h	2 m^3 / h
absolute temperature of emissions	333.2 K	313.2 K

Table 5: Determination of NO_x to SO_2 ratio to derive the SO_2 from the NO_x background map. For each of the four stations with continuous measurements, the 10% (i.e. 876 hours) of the hourly values with the lowest recorded concentration have been used.

Station	**station group**	**mean of lowest 10% hourly conc. values**		**Factor NO_x to SO_2**
		NO_x	**SO_2**	
Schwamendingen	Q1	22.1	1.2	18.7
Kaserne	Q2	20.8	1.7	12.1
Wiedikon	Q3	41.2	7.6	5.4
Stampfenbach	Q3	24.4	4.5	5.4

Table 6: Model prediction performance for 'urban' and 'non-urban' model set-up and meteorological preprocessor. For definition of FB, NMSE, COR, FAC2, see text.

	Approach	station group	NMSE	FB	COR	FAC2
Observations			0.000	0.000	1.000	100%
NO_x	'urban'	all	0.144	0.201	0.845	93%
		Q1	0.042	0.075	0.750	100%
		Q2	0.033	0.063	0.730	100%
		Q3	0.176	0.322	0.780	80%
	'non-urban'	all	0.355	0.465	0.870	82%
		Q1	0.229	0.395	0.616	90%
		Q2	0.145	0.338	0.728	100%
		Q3	0.372	0.548	0.884	60%
SO_2	'urban'	all	0.051	0.027	0.770	100%
		Q1	0.026	–0.062	0.776	100%
		Q2	0.078	0.035	0.592	100%
		Q3	0.050	0.082	0.656	100%
	'non-urban'	all	0.113	0.260	0.821	96%
		Q1	0.055	0.184	0.779	100%
		Q2	0.119	0.256	0.669	88%
		Q3	0.128	0.311	0.759	100%

Table 7: Share of different source categories in the total emission and corresponding contribution to predicted surface concentrations (arithmetic mean over all station locations, without the background concentration).

	Share in annual emission				Contribution to surface conc.			
	SO_2		NO_X		SO_2		NO_X	
	[t/a]	[%]	[t/a]	[%]	[µg/m³]	[%]	[µg/m³]	[%]
heating/industrial	1905	93.5%	1960	38.1%	14.2	81.0%	12.8	16.2%
traffic	132	6.5%	3189	61.9%	3.3	19.0%	66.6	83.8%
sum	*2037*	*100.0%*	*5149*	*100.0%*	17.5	100.0%	*79.5*	*100.0%*

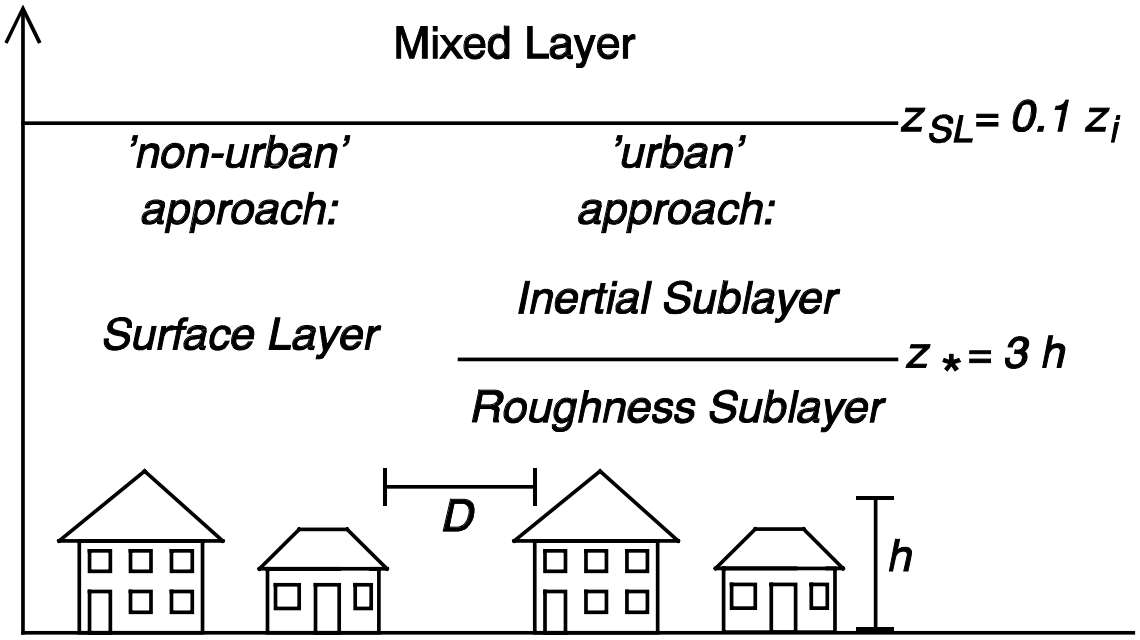

Figure 1 Conceptual sketch of the lowest layers within the boundary layer over an urban surface. The left hand side of the figure shows the situation as it is conventionally used in applied dispersion models ('non-urban' in the present terminology), while the right hand side depicts the actual situation with a roughness sublayer adjacent to the surface (referred to as 'urban' in the text). The height of the roughness sublayer is chosen as three times the average building height *h* for this study (see text for more details).

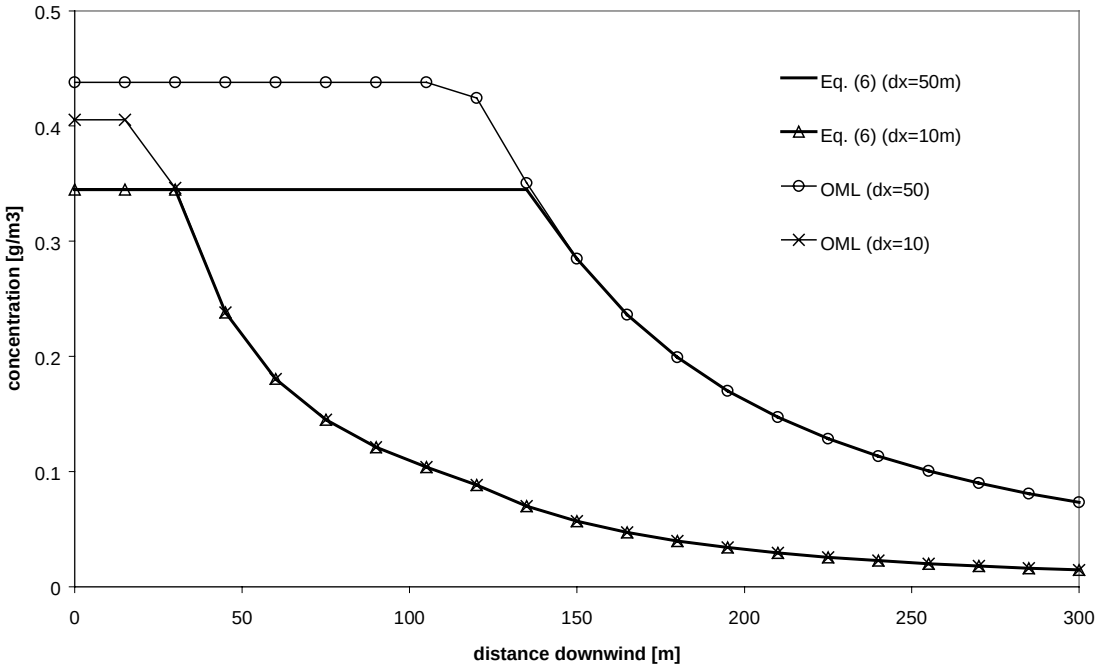

Figure 2: Effect of the upper limit on near-source concentration *C* for area sources. *dx* denotes the source size in down-wind direction. Comparison of the regular OML area source scheme (limiting $\sigma_z(x)$ by *dx*) and Eq. (6) (limiting *C* by the normalized emission rate). PGT dispersion coefficients and wind profile power law exponents taken from Hanna (1982, p. 289–293). Example for class C stability, urban conditions, roughness length 1 m, $U(z=10\text{ m}) = 4$ m/s, receptor height 2 m above ground, ground-based source with uniform emission rate 1 g/s/m^2. Lateral (cross-wind) size of the area source is 50 m for all cases.

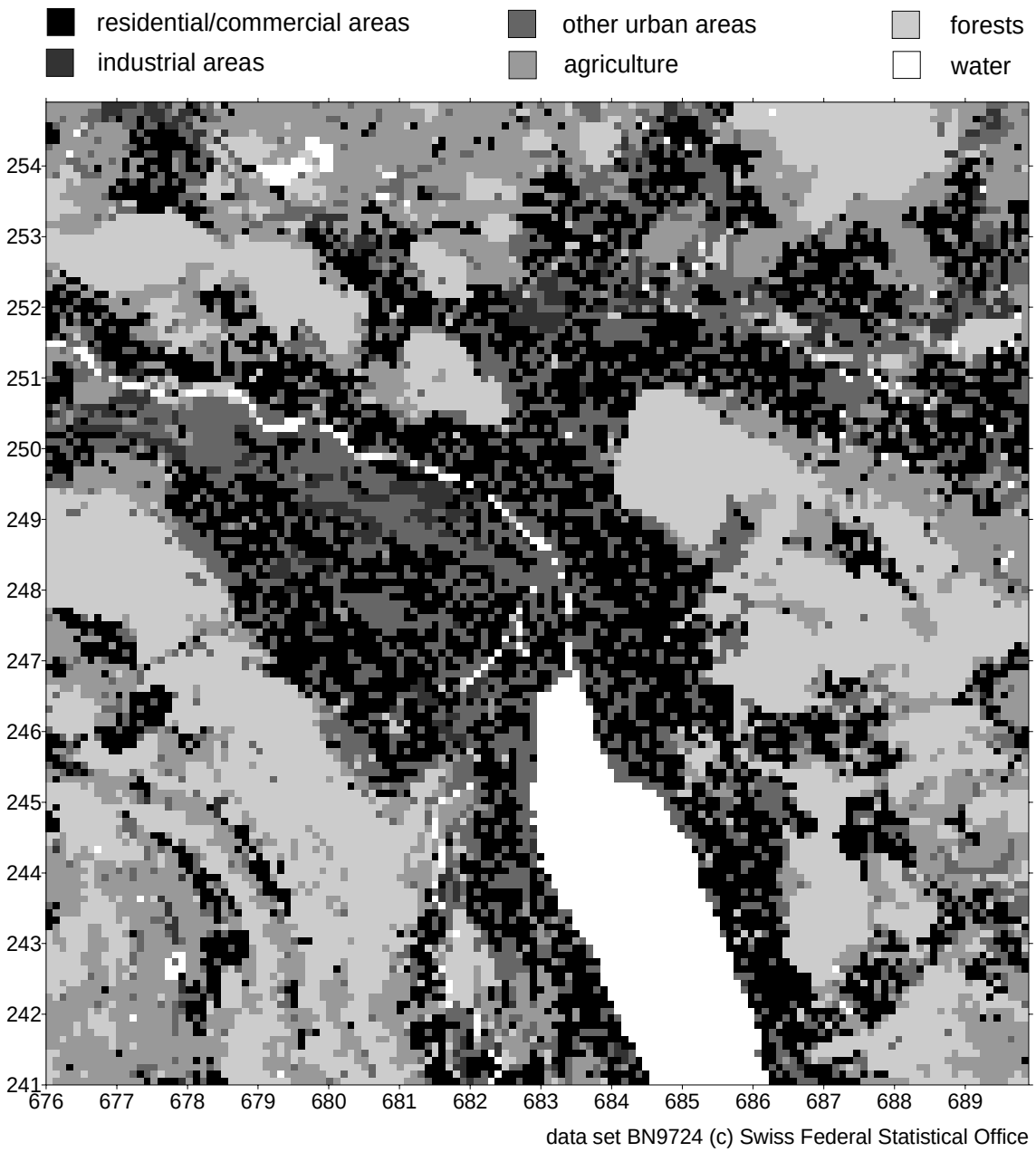

Figure 3 Land use (100 x 100 m^2 resolution; south-north and east-west axes use the Swiss coordinate system with 1 km spacing) of the city of Zurich and its surroundings, aggregated into six main categories. The city center is roughly situated at the transition of the Lake of Zurich (southern part of the figure) to the Limmat river.

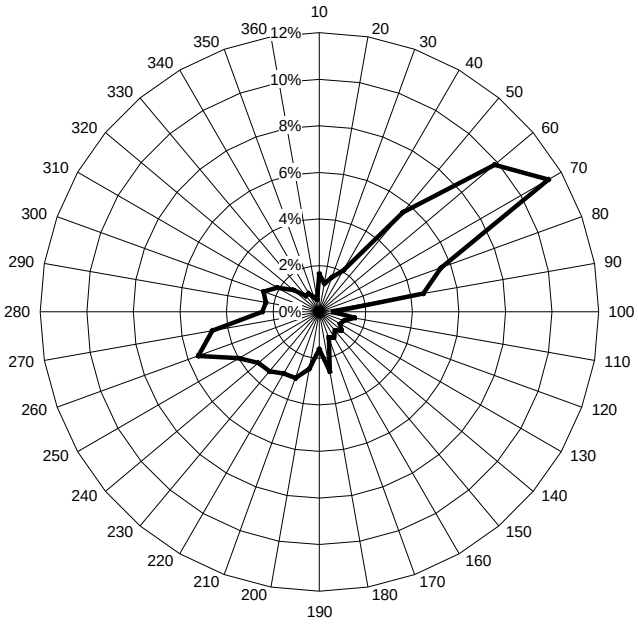

Figure 4 Wind rose of all hours of observed wind direction for 1990 at the meteorological station of the Swiss Meteorological Service in Zurich.

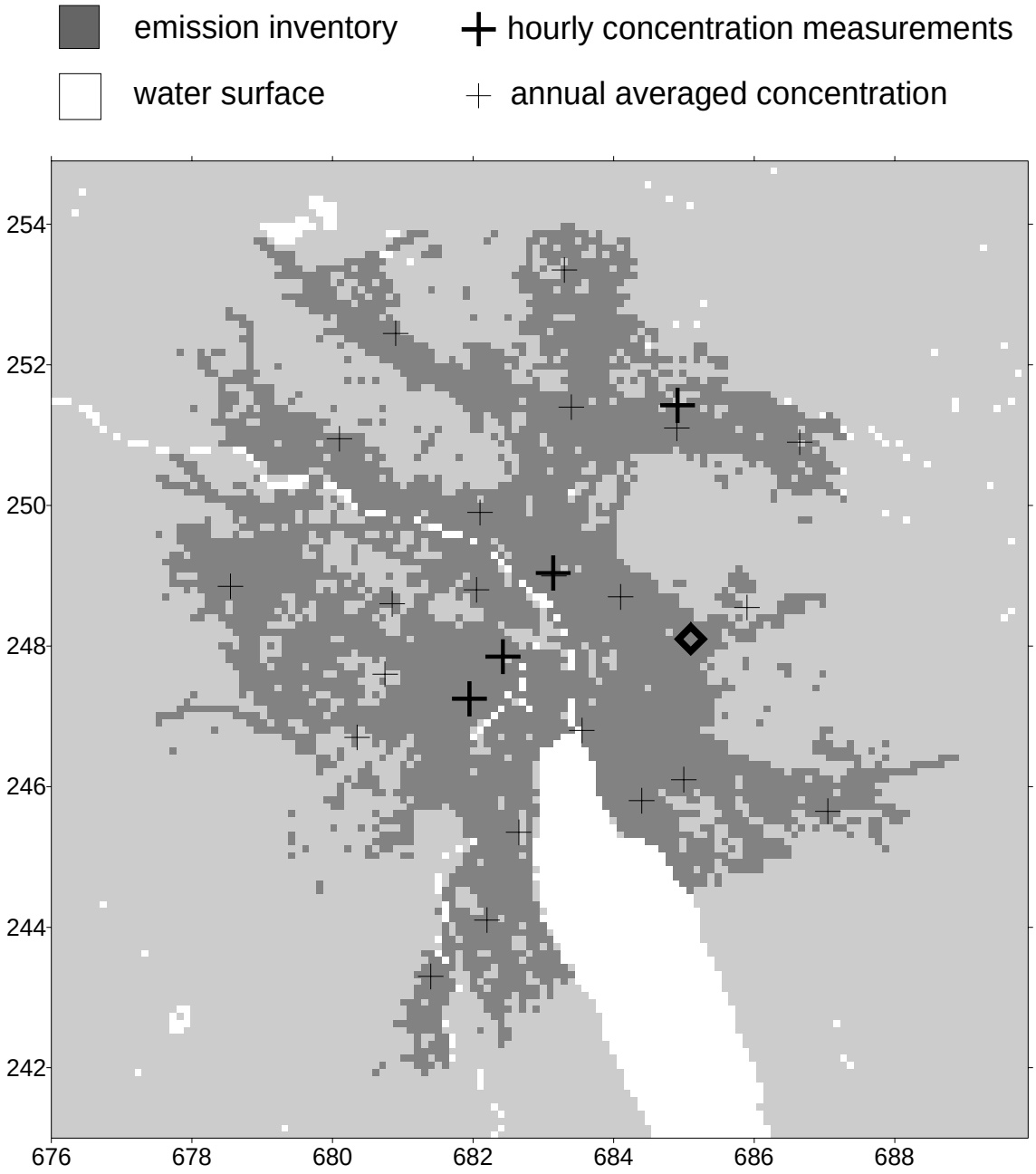

Figure 5 Location of air pollution monitoring stations and spatial extension of the emission inventory with 100 m x 100 m resolution (for 1990). The location of the national weather service meteorological station is denoted by '◆'.

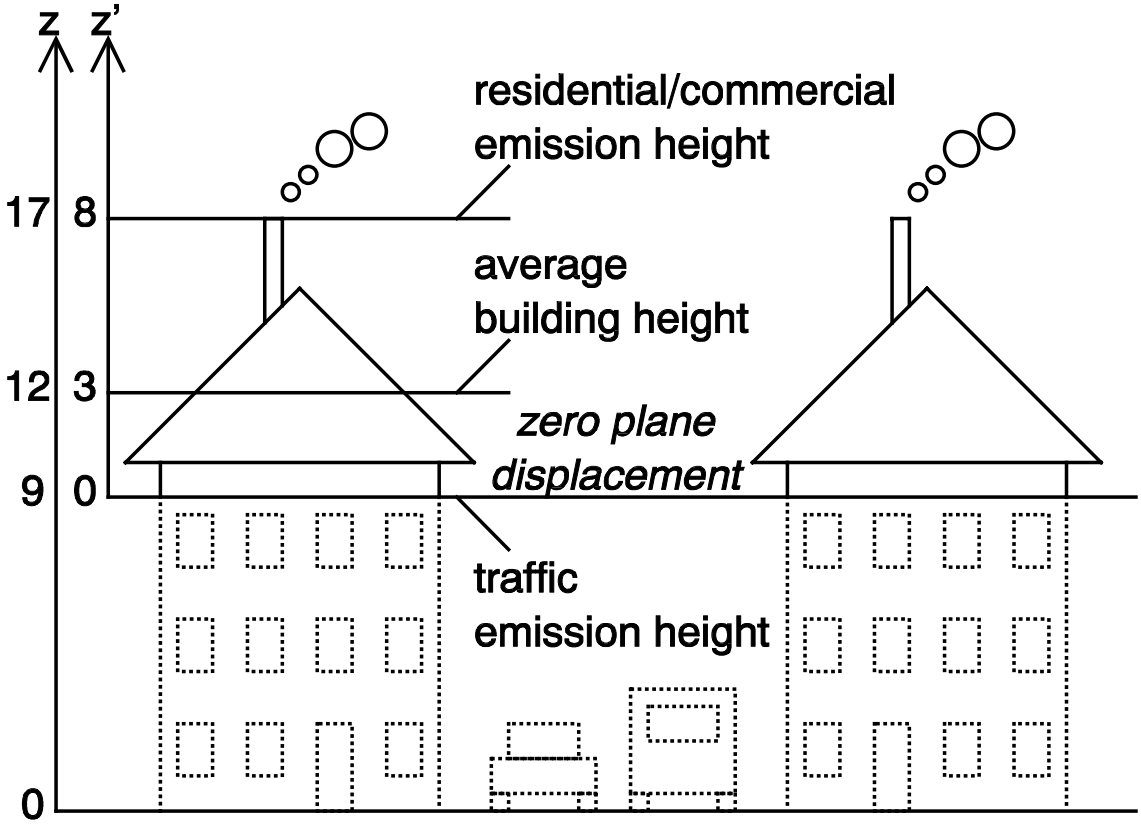

Figure 6: Set-up of the OML model for the simulation of the city of Zurich. The lower model boundary has been set to the zero plane displacement height, which is set to three quarters of the average building height. Traffic emissions are released at the bottom of the model domain. Receptor height for concentration prediction is $z' = 0$. For further explanations see text.

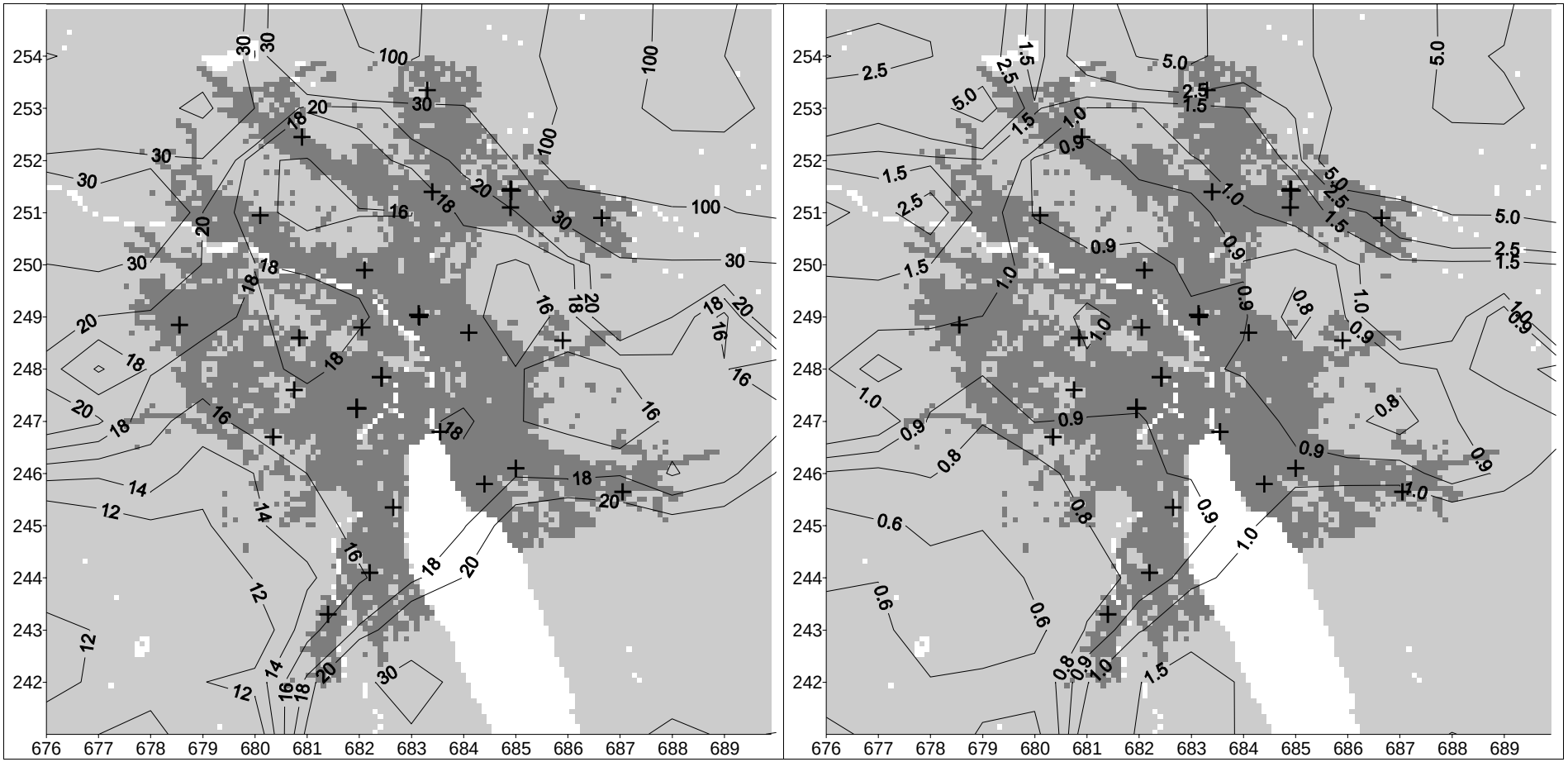

Figure 7: Background concentration maps (being the sum of the natural background concentration and the impact of all emission sources outside of the emission inventory domain) for NO_x (left panel) and SO_2 (right panel) for 1990. Annual averaged concentration in $\mu g\ m^{-3}$.

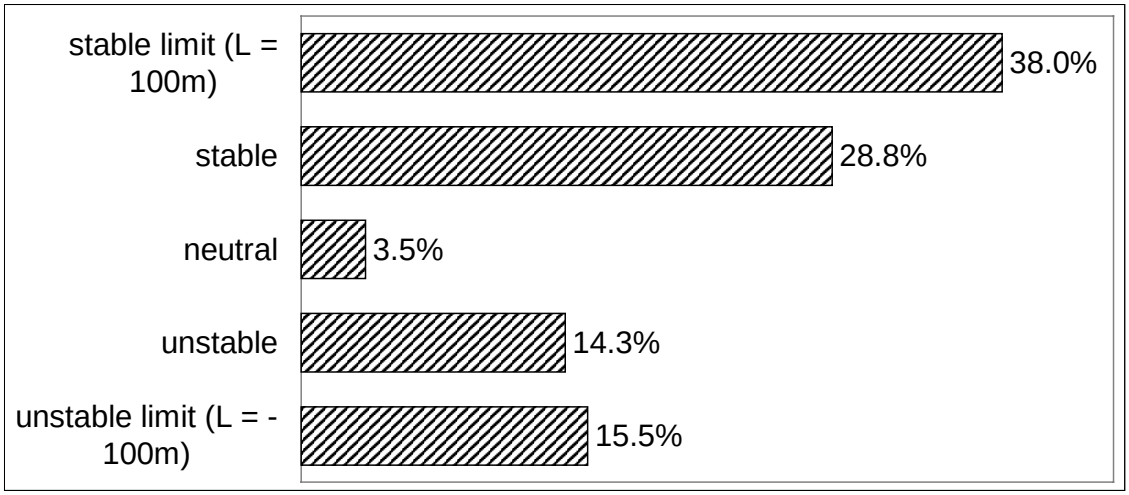

Figure 8: Effect of the lower limit on the absolute value of the Obukhov length of 100 times z_0, where z_0 = 1 m in this study.

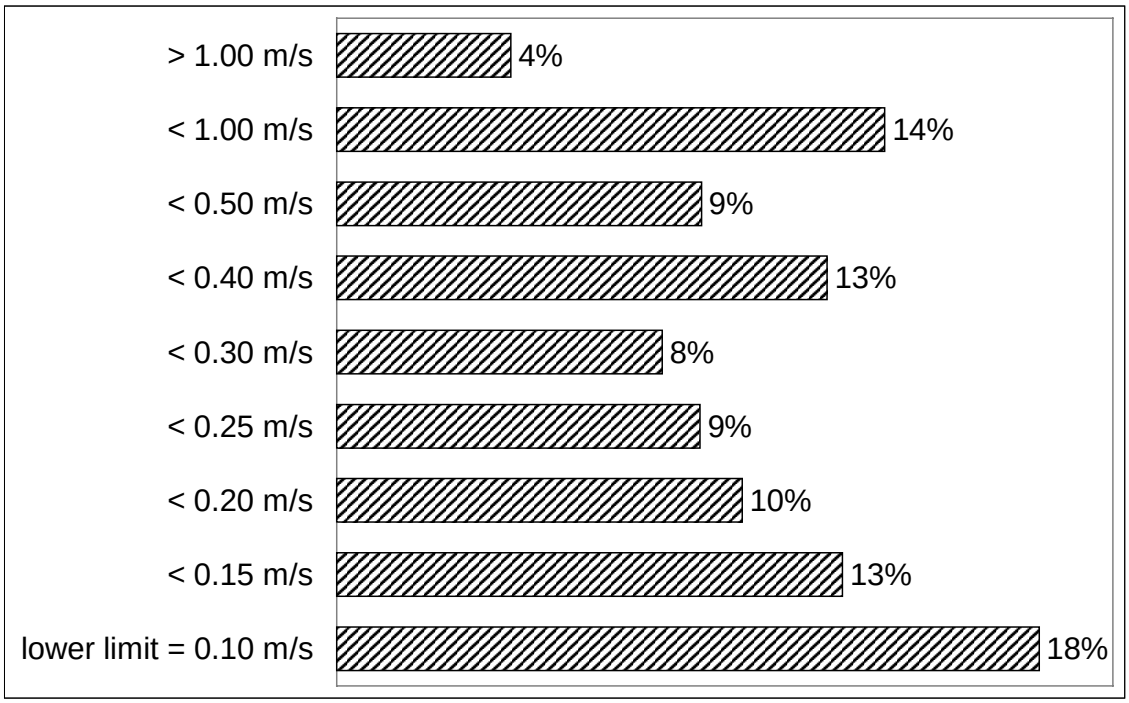

Figure 9: Classification of the roughness length u_*. The lowest limit in urban areas has been supposed to be 0.1 m s^{-1}.

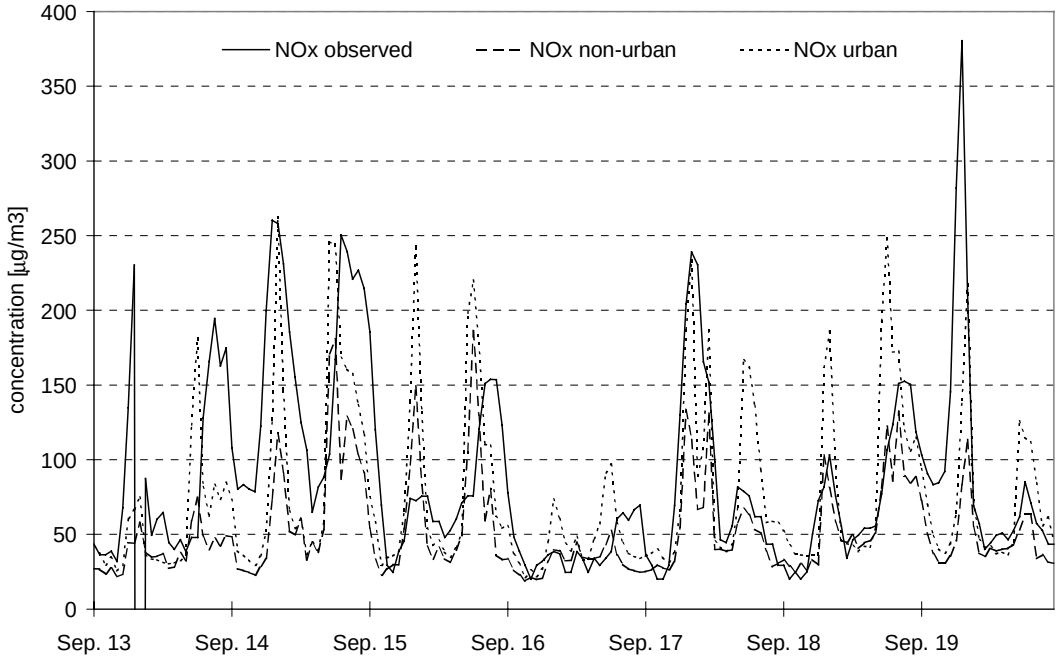

Figure 10: Example of hourly concentration data for NO_x for the location "Kaserne". The measured concentration (hourly averages) as well as OML model predictions with an 'urban' and a traditional 'non-urban' set-up are depicted.

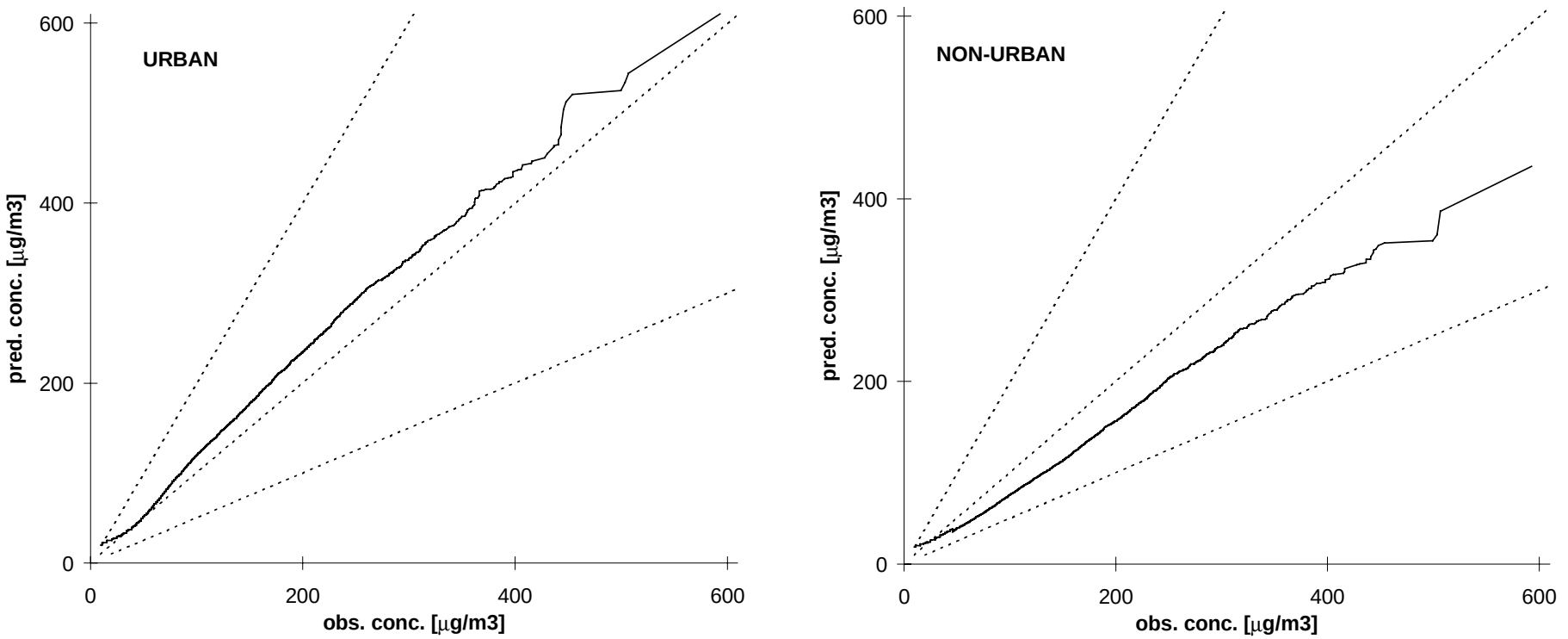

Figure 11: Quantile-quantile plot of hourly NO_x-concentrations at the location "Kaserne" for "urban" and "non-urban" model simulations. The upper and lower dashed lines indicate the range of predictions within a factor of two of observations.

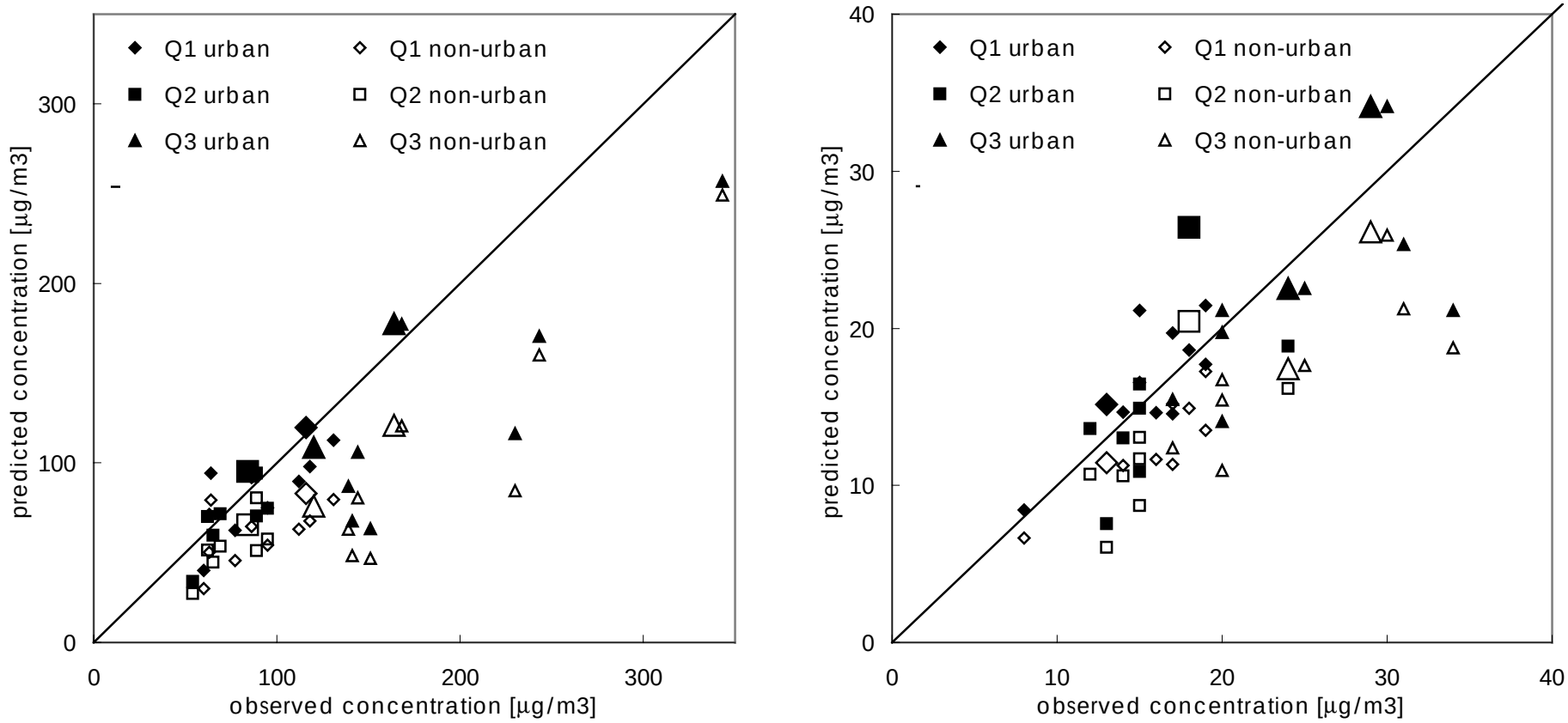

Figure 12: Scatter plot of yearly average concentration; left panel: NO_x; right panel: SO_2. Model predictions are depicted for "urban" and "non-urban" model simulations. Enlarged symbols mark those stations for which continuous (hourly) measurement data are available.